Int J Adv Manuf Technol (2017) 91:4033–4041
DOI 10.1007/s00170-017-0085-8

ORIGINAL ARTICLE

The effects of cutting parameters and tool geometry on cutting forces and tool wear in milling high-density fiberboard with ceramic cutting tools

Zhaolong Zhu[1] · **Xiaolei Guo**[1] · **Mats Ekevad**[2] · **Pingxiang Cao**[1] · **Bin Na**[1] · **Nanfeng Zhu**[1]

Received: 1 November 2016 / Accepted: 16 January 2017 / Published online: 3 February 2017

Abstract In this paper, the effects of cutting parameters and tool geometry on cutting forces and tool wear when up-milling high-density fiberboard with alumina ceramic cutting tools were investigated. Under the condition of the same feed per tooth, average chip thickness, and clearance angle, the results shown are as follows: first, the tangential forces F_t and normal forces F_r at low-speed cutting were higher than those at high-speed cutting, but increased slowly with the increase of cutting length and rake angle decrease. Second, increased cutting speed and decreased rake angle had a great effect on rake face wear. Third, the wear patterns of tool wear were rake wear and flank wear, which included pull-out of grain, flaking, and chipping. The wear mechanisms were adhesive wear and abrasive wear. Finally, at low-speed cutting, the cutting tools with bigger rake angle can be selected to reduce the energy consumption of machine tools. The tools with smaller rake angle can be used for high-speed cutting to improve tool life and productivity of processing.

✉ Xiaolei Guo
youngleiguo@hotmail.com

Zhaolong Zhu
njfuzzlong@163.com

[1] Faculty of Material Science and Engineering, Nanjing Forestry University, Nanjing, Jiangsu, China

[2] Division of Wood Science and Engineering, Luleå University of Technology, Skellefteå, Sweden

Keywords Ceramic cutting tool · High-density fiberboard · Cutting forces · Tool wear

1 Introduction

Subject to resource constraints, traditional culture, development of science and technology, furniture design, and so on, the age of furniture materials has changed from a single wood to composite materials. But no matter how the furniture materials have evolved, wood materials have always taken the dominant position of furniture materials. Among the furniture materials, high-density fiberboard (HDF) has been used widely, because of its fine texture, stable performance, strong grip nails, well resistance to deformation, and surface decoration [1].

With the widespread application of HDF, CNC working centers are widely used, especially when high quality of product and flexibility of manufacturing process are expected [2]. Most processing methods have been conducted, such as milling, planning, routing, and sanding [3]. Among them, milling is the most commonly used for wood processing, which has posted great challenges to the wood-processing industry. Nowadays, the cemented carbide cutting tools were used in wood processing frequently. Though they can provide a good ratio of hardness and fracture toughness [4], the cemented carbide cutting tools cannot meet modern wood processing. The reasons are as follows: first, the wood cutting processing is very complicated, because cutting speed is 5–20 times higher than conventional metal, and the high density of cemented carbide cutting tools may be dangerous in high-speed cutting [5]. Then, wood materials are anisotropic and inhomogeneous, which contain knots and silicates. Last, the tannins and adhesive in the wooden products are easy to corrode cemented carbide cutting tools [6]. Above all, they all

shorten the lifetime of cutting tools and decrease the efficiency of industrial production. Aimed at the higher efficiency, some enterprises have tried to use diamond cutting tool, but its high price seriously raises production costs [7]. All those attract our attention to the ceramic cutting tools naturally.

Due to the poor toughness of ceramic materials that are usually based on oxide components, ceramic cutting tools have been limited in the wood processing [8]. However, the development of toughening [9] has alleviated the problem of the fracture toughness of ceramic and expanded the market of ceramic cutting tools, making us see the prospects of ceramic cutting tools for wood processing. As we all know, ceramic cutting tool has the incomparable advantages to other materials. First of all, its excellent wear resistance and high hardness can expand the scope of the processing object and using life. Then, the excellent chemical stability can availably prevent chemical attack from the tannins and adhesive of wood products. Besides, its low density may offer benefits in high-speed cutting, where centrifugal forces occur, due to high spindle rotation. Last, low friction coefficient of ceramic tool is more suitable for high-speed wood processing [10–12]. The first study of alumina-based ceramic cutting tools was Gogolewski [9], who showed the main wear of ceramic cutting tools was chipping. Then, a further study made by Eblagon [12] showed that the lifetime of ceramic cutting tools was much longer than cemented carbide cutting tools. Huang studied the milling properties of compressed wood, which showed that the horizontal cutting forces increased with the increase of compression and cutting depth, but decreased with rake angle increase [13]. Claudia Streher [5] found the recession of the Si_3N_4/SiC cutting tools was less than one half of the minimum edge recession of the cemented carbide cutting tools by measuring the edge recession after the lifetime cutting test. Kumar's results showed the wear patterns of alumina-based ceramic cutting tools in machining hardened martensitic stainless steel were flank wear, crater wear, and notch wear [14]. Guangming Zheng identified the wear mechanisms of ceramic cutting tools in the machining tests involved adhesive wear and abrasive wear [15]. The most important research was carried by Forni [16], who found Si_3N_4-based ceramic matrix composites have the potential to become a tool material for wood processing with the deepening of multiple experiments.

Though the research and application of ceramic cutting tools are sufficient in metal processing [17], the domestic and international research on ceramic cutting tools in wood processing is still relatively limited [18]. In order to provide theoretical basis of the use of ceramic cutting in wood processing, in this paper, three different geometry ceramic cutting tools were used in milling the HDF at different cutting speeds, and the purpose of this experiment is to study the influence of tool geometry and cutting parameters on cutting forces and tool wear.

2 Experiment

2.1 Ceramic cutting tools

The TiC-reinforced Al_2O_3 ceramic cutting tools made by Kyocera Trading Co. Ltd. in China were used in this milling test. The cutter carried six inserts each with a diameter of 100 mm to maintain a constant cutting condition. Figure 1 and Table 1 show the tool geometry parameters and mechanical properties of ceramic cutting tools.

2.2 Workpiece materials

The milling objects were HDF (Power Dekor Group Co. Ltd. China), which were made of raw materials comprising of pine and poplar wood fiber, with the addition of the adhesive of urea-formaldehyde resin catalyzed by ammonium chloride. The average density, modulus of elasticity (MOE), and modulus of rupture (MOR) of the HDF are 861 kg/m^3, 4312, and 49.7 MPa, respectively (Table 2). The HDFs were rectangular blocks, whose dimensions were 150 (length) × 80 (width) × 10.7 (depth) mm.

2.3 Experimental design

In this paper, the cutting forces and tool wear were tested by up-milling on the CNC (MGK01A, Nanxing Group Co. Ltd., China). As shown in Fig. 2, HDF samples were mounted on the dynamometer, which transmitted the signal to a charge amplifier. Then, the charge was transferred from the amplifier to the A/D transducer that would transmit the signal to the computer, on which the specific data can be seen. The cutting

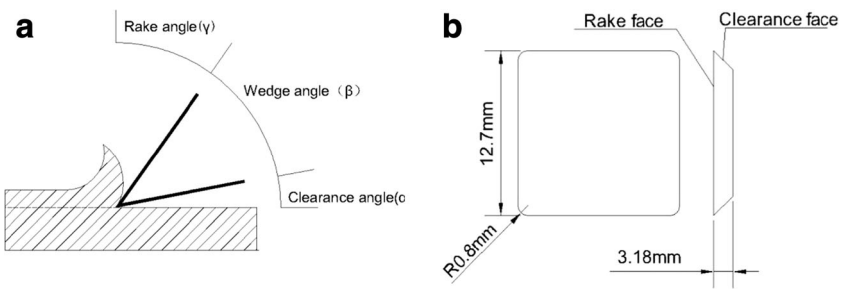

Fig. 1 The model of ceramic cutting tools. **a** The parameters of angle. **b** The parameters of size

Table 1 The geometry parameters and mechanical properties of tools

Ceramic cutting tools	Mechanical properties				Structure parameters		
	Chemical composition	Hardness/GPa	Flexural strength/MPa	Toughness/MPa	Rake angle (°)	Wedge angle (°)	Clearance angle (°)
Tool A	Al_2O_3 + TiC	20.1	980	4.1	6	79	5
Tool B					10	75	5
Tool C					15	70	5

forces of three-axis directions (F_x, F_y, F_z) were measured, where the direction of F_x was paralleled to the feed speed, the direction of F_y was perpendicular to the feed speed, and the F_z was normal direction of the panel of F_x and F_y. Because the cutting tools used straight cutting edges, F_z was almost zero and would not be considered as specialized problems. As shown in Fig. 3, for a better study of cutting forces, the tangential forces (F_t) and the normal forces (F_r) were used as reference object. F_t was defined as the cutting force component perpendicular to the radius direction, and F_r was defined as the cutting force component parallel to the radius direction. The angle (θ) was defined as the angle between the direction of rotation and the direction of feed. Then, according to the measured date F_x and F_y, F_t and F_r can be obtained by conversion Eqs. 1 and 2, which are shown below.

The calculating formula of angle (θ): (1), the cutting force conversion formula of F_t and F_r: (2)

$$\theta = \arcsin\sqrt{\frac{h}{D}} \tag{1}$$

$$\begin{pmatrix} F_t \\ F_r \end{pmatrix} = \begin{pmatrix} \cos\theta & -\sin\theta \\ \sin\theta & \cos\theta \end{pmatrix} \begin{pmatrix} F_x \\ F_y \end{pmatrix} \tag{2}$$

where h = 1 is the cutting depth (mm), D = 100 is the tool diameter (mm), and $\sin\theta = 0.1$ and $\cos\theta = 0.995$.

In this paper, scanning electron microscope (SEM) and energy-dispersive spectroscopy (EDS) were used to quantify tool wear, and the wear patterns and wear mechanism of ceramic tools were obtained by observing the wear morphology and analyzing the elements.

With three different rake angles of cutting tools, as shown in Table 2, experiments were performed at two different cutting speeds, shown in Table 3. It is worth mentioning that although this experiment chose two different cutting speeds, namely a high-speed cutting and low-speed cutting, the average thickness of chip and feed per tooth of two cutting speeds are identical. Eqs. 3 and 4 and Fig. 4 show how the average chip thickness and feed per tooth were obtained in different ways where the cutting depth was 1 mm, the cutting diameter was 100 mm, and the number of teeth was six. In other words, the same average chip thickness and feed per tooth were attained by combination of the low spindle and feed speed in a low-speed cutting condition and the high spindle and feed speed in a high-speed cutting condition. The aim of this experimental design was to study the effect of tool geometry and cutting speed on cutting forces and tool wear under the condition of the same average thickness of chip, feed per tooth, and clearance angle.

Table 2 The physical and mechanical properties of HDF (the content in parentheses is the standard deviation of MOE, MOR, and density calculated from 10 data of the sample HDF)

Sample	Density (kg/m^3)	MOE (MPa)	MOR (MPa)
HDF	861 (1.07)	4312 (1.43)	49.7 (0.92)

The formulas of feed per tooth and average chip thickness are as follows:

$$U_z = \frac{U}{n{\cdot}z}\,(\text{mm}) \tag{3}$$

$$a_{\text{av}} = \frac{U}{n{\cdot}z}\sqrt{\frac{h}{D}}(\text{mm}) \tag{4}$$

where U_z is feed per tooth (mm), a_{av} is average chip thickness (mm), U is feed rate (mm/min), Z is number of teeth, n is rotation speed (rpm), h is cutting depth (mm), and D is tool diameter (mm).

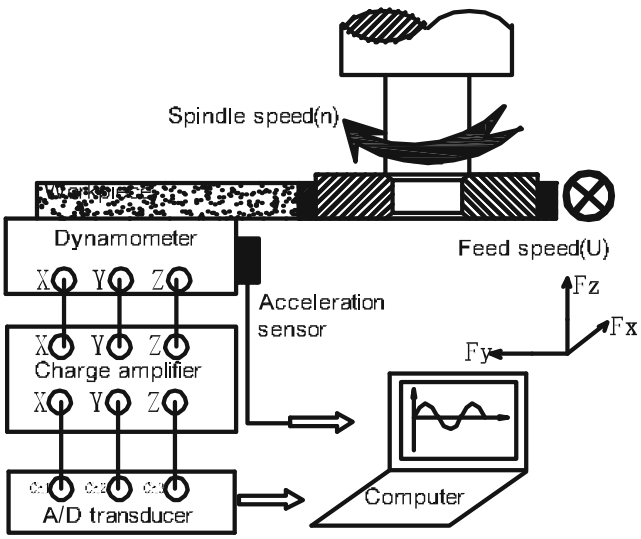

Fig. 2 The schematic diagram of cutting force measuring system

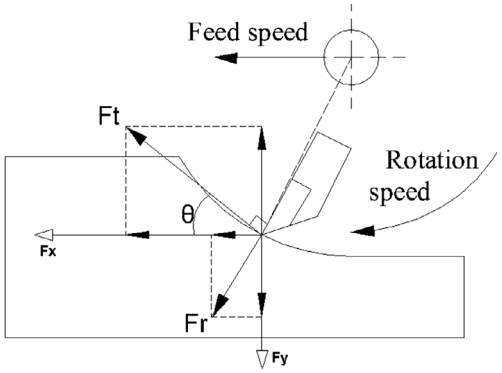

Fig. 3 The schematic diagram of cutting forces

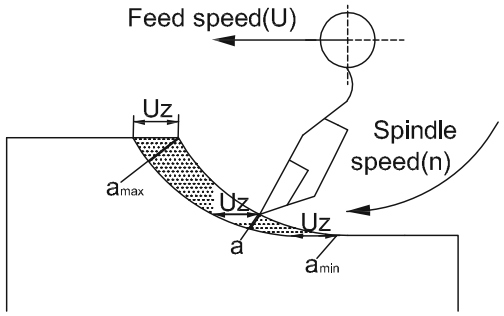

Fig. 4 The model diagram of cutting parameters

3 Result and discussion

3.1 Cutting forces

Cutting force, a crucial parameter for tool design, has a direct effect on power consumption, cutting heat, tool wear, and the quality of machined surface [19], whereas the effects of workpiece material, cutting thickness, friction, tool geometry, and cutting parameters on cutting force are significant [20]. This paper studied the influence of tool geometry and cutting parameters on cutting forces under condition of the same feed per tooth, average chip thickness, and clearance angle.

3.1.1 The influence of cutting length on cutting forces

Figure 5 shows the trends of F_t and F_r with cutting length. Whether at low-speed or high-speed cutting, F_t and F_r increased slowly with cutting length increasing. The increase of F_t and F_r was due to the tool wear, which mainly came from two aspects. One was the increase of resistance in separating chips from workpiece, because in HDF processing, the wear on cutting edge increased gradually, and even breakage might appear. The other was the more serious friction between the tool face and HDF, which all led to the increase of cutting forces.

3.1.2 The influence of cutting speed on cutting forces

As shown in Fig. 6, the influence of cutting speed on F_t and F_r is relatively obvious, which reveals that F_t and F_r at low-speed cutting were higher than F_t and F_r at high-speed cutting. As mentioned above, high-speed cutting contained high feed speed and spindle speed, in unit time; the friction frequency between tool and workpiece increased with cutting speed increasing, and it led to the increase of cutting temperature in contact zone; then, the friction coefficient decreased with cutting temperature increasing, which led to cutting force decrease. Therefore, F_r and F_t at low-speed cutting were higher than those at high-speed cutting. So, the high cutting speed could not only decrease cutting force and energy consumption but also improve the productivity of processing.

3.1.3 The influence of tool geometry on cutting forces

Figure 7 shows the influence of tool geometry on cutting forces, which reveals whether at low-speed cutting or high-speed cutting, F_r and F_t decreased with the increase of rake angle. Because the bigger rake angle means the smaller wedge angle and the shaper cutting edge, it was more likely to cut the fiber and glue of HDF. Besides, the acting forces between chips and rake face decreased with rake angle increase. Hence, F_r and F_t decreased with the increase of rake angle. If tool strength is insured, the greater the rake angle, the

Table 3 The design of the same average chip thickness value can be reached either by changing the feed rate at low rotation speed (left) or by changing the feed rate at high rotation speed (right)

Test number	Low-speed cutting		a_{av} (mm)	Tools	h (mm)	Cutting length (m)	High-speed cutting		Test number
	n (r/min)	U (mm/min)					n (r/min)	U (mm/min)	
1	5000	30,000	0.1	A/B/C	1	0	10,000	60,000	7
2	5000	30,000	0.1	A/B/C	1	5	10,000	60,000	8
3	5000	30,000	0.1	A/B/C	1	10	10,000	60,000	9
4	5000	30,000	0.1	A/B/C	1	15	10,000	60,000	10
5	5000	30,000	0.1	A/B/C	1	20	10,000	60,000	11
6	5000	30,000	0.1	A/B/C	1	25	10,000	60,000	12

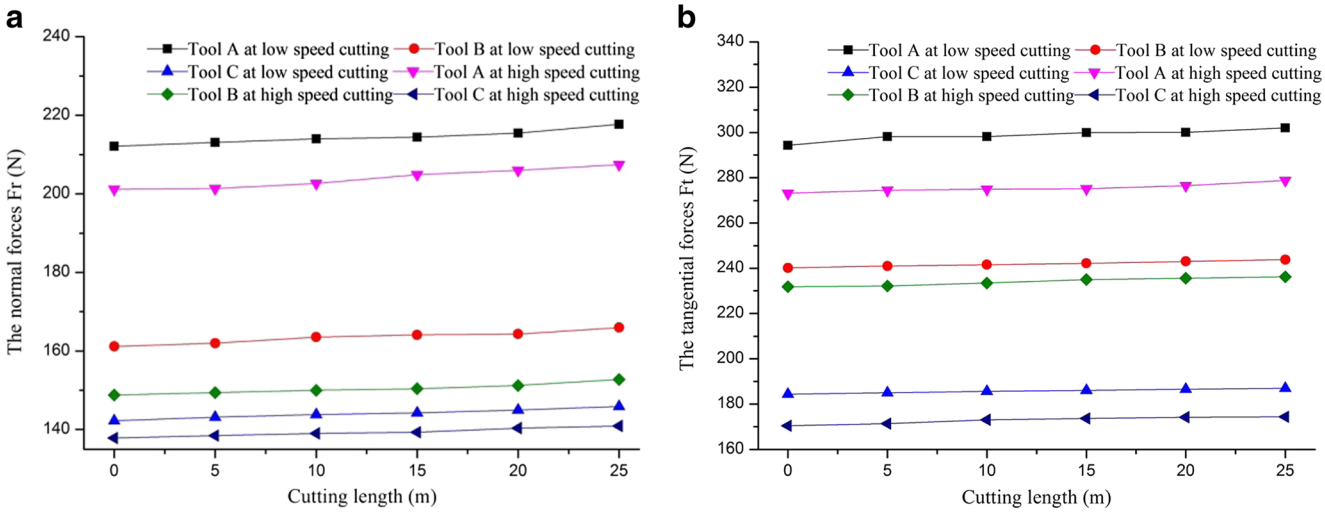

Fig. 5 The influence of cutting length on cutting forces. **a** The change of F_r. **b** The change of F_t

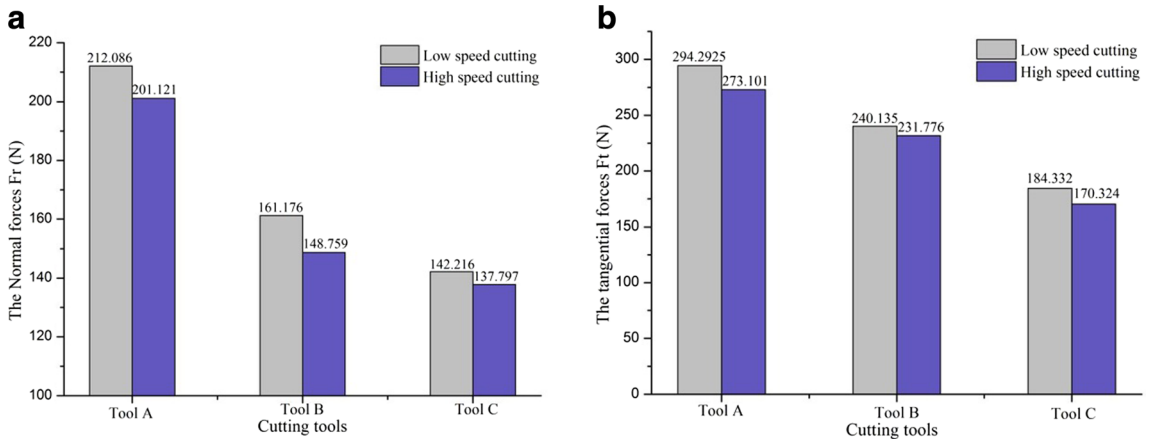

Fig. 6 The influence of cutting speed on cutting forces. **a**. The comparison of F_r. **b** The comparison of F_t

smaller the cutting force, it is more conducive to reducing energy consumption of machine tool.

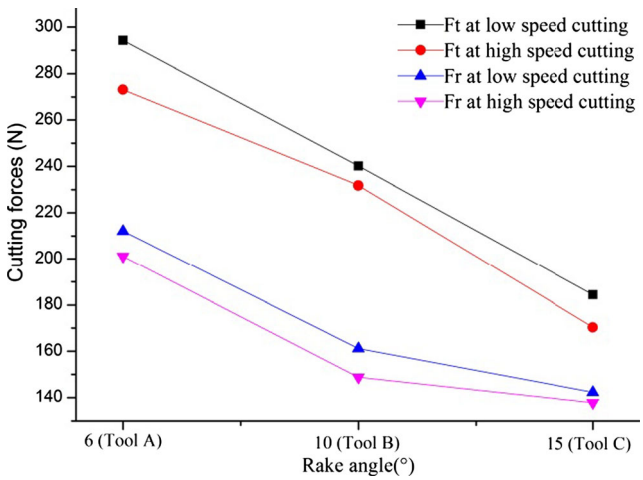

Fig. 7 The influence of tool geometry on cutting forces

3.2 Tool wear patterns

The wear patterns of alumina ceramic cutting tools were primarily divided into rake face wear and flank wear, where the former is always accompanied by flaking, chipping, crack, and even breakage [21]. In this paper, under condition of the same feed per tooth, average chip thickness, and clearance angle, the influence of cutting parameter and tool geometry on tool wear was discussed.

3.2.1 Rake wear

As shown in Figs. 8 and 9, due to the extrusion and friction between chips and rake face in the cutting process, some significant wear could be observed on the rake face, such as pull-out of grain, flaking, and chipping. The reason for pull-out of grain and flaking was the cutting forces increasing, which led the increase of extrusion and friction between chips and rake face. Then, as the cutting temperature increased with cutting

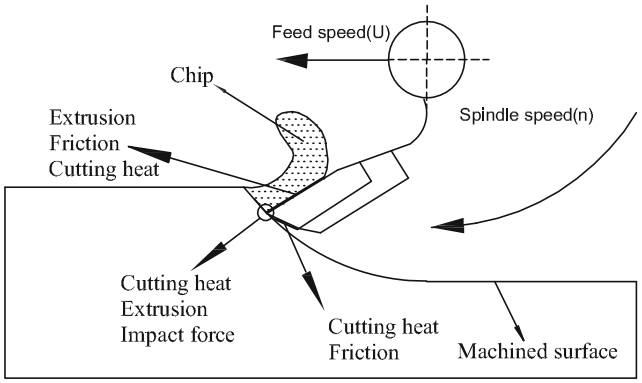

Fig. 8 Model diagram of tool wear

forces increasing, the workpiece material was adhered to the tool surface. When the bond material fell off under mechanical and thermal shock, it led to pull-out of grain and flaking. What led to chipping was that, in the early stage of cutting, the cutting edge was relatively sharp. When the new cutting edge cuts HDF, the concentrated stress led to chipping. Even when crashing to the hard particles, it was easy for the instantaneous impact force to produce chipping as well.

By comparing a and d, b and e, and c and f, the influence of cutting speed on rake face can be seen clearly, where tool wear at high-speed cutting was more serious than tool wear at low-speed cutting; because the high cutting speed included high feed speed and spindle speed, it increased the processing capacity in unit time, which brought more cutting heat and acting force to rake face. Besides, in high-speed cutting processing, when encountering hard particles that produced more impact forces, it is more likely to cause wear, even breakage. Therefore, the high-speed cutting condition had a great influence on rake face wear, where the bigger rake angle tools can be chosen to reduce wear.

By comparing a, b, and c, and d, e, and f, the influence of cutting speed on rake face wear can be seen clearly, where the rake face wear increased with the decrease of rake angle, because in the same clearance angle, the smaller rake angle means the bigger wedge angle and blunter cutting edge, which was more difficult for the tool to cut the fiber and glue in HDF. In addition, the smaller rake angle led to the bigger power consumption, where the most obvious is that the deformation coefficient of chip, as depicted in Fig. 10, decreased distinctly with the rake angle increasing. If tool strength is insured, the tool with larger rake angle can effectively reduce the rake face wear to improve the tool life.

3.2.2 Flank wear

According to Fig. 10, it is the intense friction and cutting heat occurred between the workpiece surface and flank face that cause flank wear. Due to the same clearance angle, the acting force of the machined surface on the flank shows almost no difference and the flank wear is similar. From Fig. 11, it can be seen that there are many intensive scratches on the flank face, which is the typical abrasive wear.

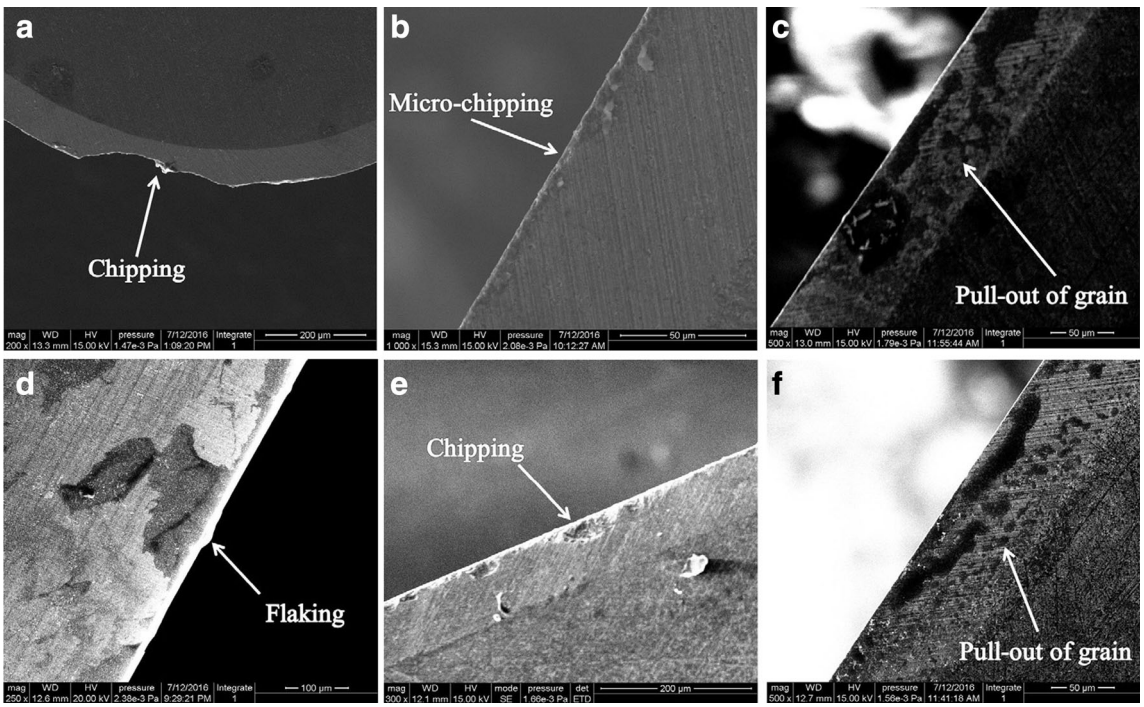

Fig. 9 Rake face wear map of cutting length in 25 m. **a** Tool A at low-speed cutting. **b** Tool B at low-speed cutting. **c** Tool C at low-speed cutting. **d** Tool A at high-speed cutting. **e** Tool B at high-speed cutting. **f** Tool C at high-speed cutting

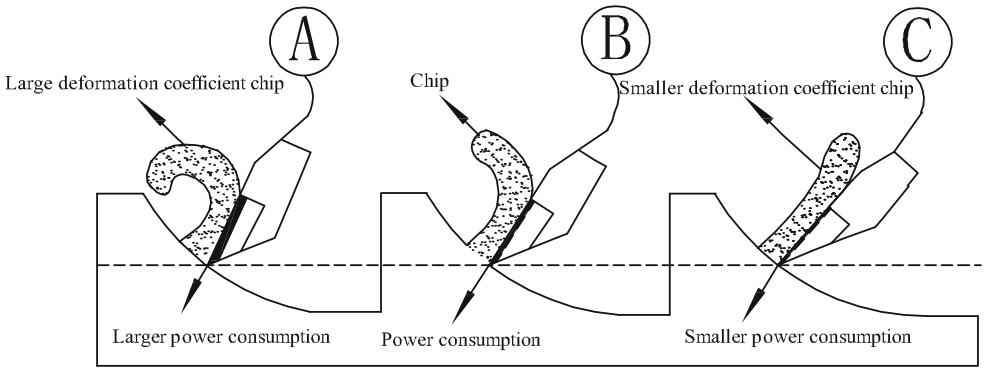

Fig. 10 The analysis diagram of rake face wear

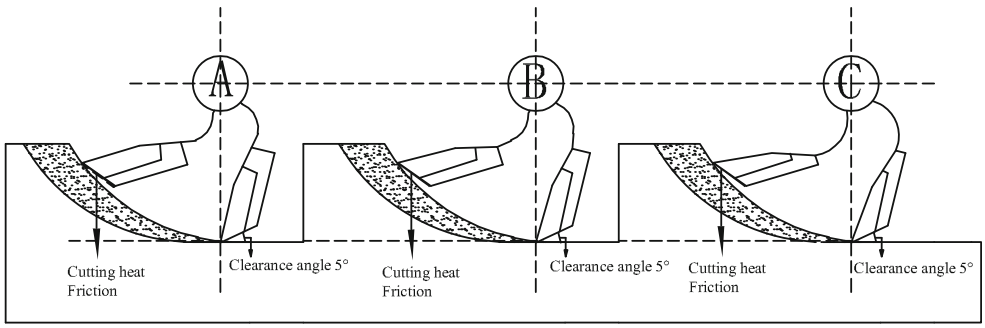

Fig. 11 The analysis diagram of flank wear

3.3 Wear mechanism

The wear mechanism of SiAlON ceramic tools was studied by Tian [22], whose research showed the wear mechanism of SiAlON ceramic tools in milling Inconel 718 was adhesive wear. To understand tool wear mechanism in milling HDF better, SEM and EDS were used to study the wear mechanism, and the results showed that the main wear mechanisms were adhesive and abrasive wear.

3.3.1 Adhesive wear

Figure 12a, b shows the EDS analysis of areas a and b; the main elements contain Ti, C, Al, and O from tool material; small amounts of elements such as K, Cl, Na, and Ca were detected on surface of the tool; and none of them belong to the material elements of the tools. Because the content of K, Cl, Na, and Ca existed in only very small quantities, the same as those of adhesive curing agent, filler, catalyst, and calcium carbonate in HDF, we can conclude adhesive wear occurred. What is more, because alumina ceramic material is ionic bond and has a strong adsorption capacity [23], in the cutting process of high speed and high temperature, the workpiece material was adhered to the tool easily; when the bond material drop off, it took away some cutting tool material and eventually led to the adhesive wear.

3.3.2 Abrasive wear

As depicted in Fig. 13, many intensive scratches were observed on the flank face, which is typical abrasive wear. In the milling process, the hard particles such as adhesive curing agent, filler, and calcium carbonate generated alternate friction, which led to groove shape on the flank face.

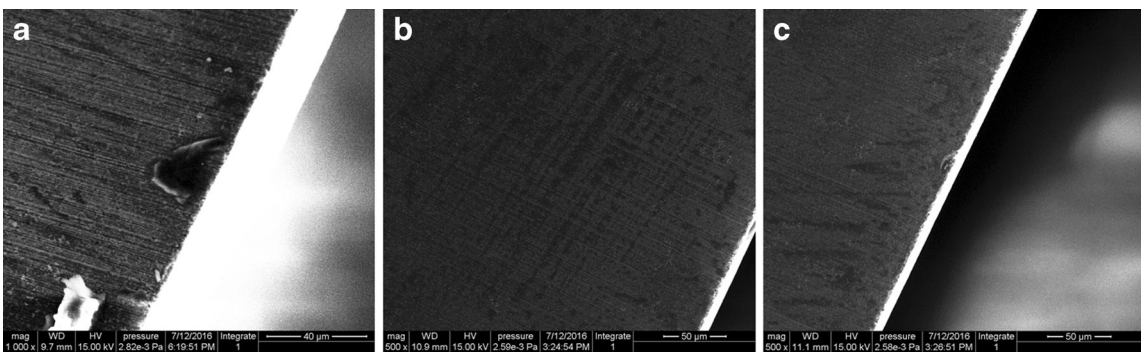

Fig. 12 The figure of flank wear topography. **a** Tool A. **b** Tool B. **c** Tool C

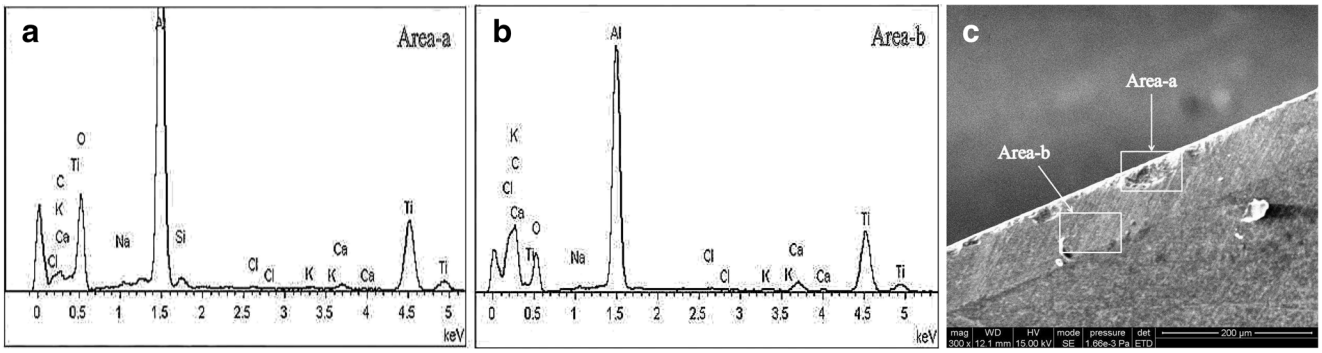

Fig. 13 The figure of flank wear topography. **a** Tool A. **b** Tool B. **c** Tool C

Furthermore, the alumina ceramic cutting tools were toughened by TiC, which grinding capacity is comparable to diamond; when it pulled out, it scratched the flank face too under the action of extrusion force.

4 Conclusion

Under the condition of the same feed per tooth, average chip thickness, and clearance angle, the conclusions of this work are as follows:

1. The tangential forces F_t and normal forces F_r at low-speed cutting are higher than those at high-speed cutting, but increased slowly with the increase of cutting length and rake angle decrease.

2. Increased cutting speed and decreased rake angle had a great effect on rake face wear.

3. At low-speed cutting, the cutting tools with bigger rake angle can be selected to reduce the energy consumption of machine tools. Then, the tools with smaller rake angle can be used for high-speed cutting to improve tool life and productivity of processing.

4. The wear patterns of alumina ceramic cutting tools are rake face wear and flank wear, which may take the patterns of pull-out of grain, flaking, and chipping. Wear mechanisms of alumina ceramic cutting tools in milling HDF are adhesive wear and abrasive wear.

Acknowledgments The authors are grateful for the support from the National Science Foundation of China (31500480), a project funded by the Priority Academic Program Development of Jiangsu Higher Education Institutions (PAPD), Kyocera for supplying the samples of ceramic cutting tools, and Power Dekor Group Co. Ltd. for supplying the samples of HDF.

References

1. Ayrilmis N (2007) Effect of panel density on dimensional stability of medium and high density fiberboards. J Mater Sci 42:8551–8557. doi:10.1007/s10853-007-1782-8
2. Gawroński T (2013) Optimisation of CNC routing operations of wooden furniture parts. Int J Adv Manuf Technol 67:2259–2267. doi:10.1007/s00170-012-4647-5
3. Saloni D, Buehlmann U, Lemaster RL (2011) Tool wear when cutting wood fiber-plastic composite materials. For Prod J 61:149–154. doi:10.13073/0015-7473-61.2.149
4. Guo X, Ekevad M, Grönlund A, Marklund B, Cao P (2014) Tool wear and machined surface roughness during wood flour/polyethylene composite peripheral upmilling using cemented tungsten carbide tools. Bioresources 9:3779–3791. doi:10.15376/biores.9.3.3779-3791
5. Strehler C, Ehrle B, Weinreich A, Kaiser B, Graule T, Aneziris CG, Kuebler J (2012) Lifetime and wear behavior of near net shaped Si3N4/SiC wood cutting tools. Int J Appl Ceram Technol 9:280–290. doi:10.1111/j.1744-7402.2011.00690.x
6. Sommer F, Kern F, Gadow R (2013) Injection molding of ceramic cutting tools for wood-based materials. J Eur Ceram Soc 33:3115–3122. doi:10.1016/j.jeurceramsoc.2013.05.012
7. Sommer F, Dan T, Kern F, Gadow R, Heisel U (2013) Medium density fiberboard machining and wear behavior of injection-molded ceramic composite wood cutting tools. Int J Appl Ceram Technol 12(147):156. doi:10.1111/ijac.12144
8. Beer P, Gogolewski P, Klimke J, Krell A (2007) Tribological behaviour of sub-micron cutting-ceramics in contact with wood-based materials. Tribol Lett 27:155–158. doi:10.1007/s11249-007-9212-2
9. Gogolewski P, Klimke J, Krell A, Beer P (2009) Al2O3 tools towards effective machining of wood-based materials. J Mater Process Technol 209:2231–2236. doi:10.1016/j.jmatprotec.2008.06.016
10. Bocanegra-Bernal MH, Matovic B (2009) Dense and near-net-shape fabrication of Si3N4 ceramics. Materials Science & Engineering A 500:130–149. doi:10.1016/j.msea.2008.09.015
11. Guo XL, Cao PX, Liu HN, Teng Y, Guo Y, Wang H (2013) Tribological properties of ceramics tool materials in contact with wood-based materials. Adv Mater Res 764:65–69. doi:10.4028/www.scientific.net/AMR.764.65
12. Eblagon F, Ehrle B, Graule T, Kuebler J (2007) Development of silicon nitride/silicon carbide composites for wood-cutting tools. J Eur Ceram Soc 27:419–428. doi:10.1016/j.jeurceramsoc.2006.02.040
13. Huang YS, Chen SS, Hwang GS, Tang JL (2003) Peripheral milling properties of compressed wood manufactured from planted China-fir. European Journal of Wood and Wood Products 61:201–205. doi:10.1007/s00107-003-0376-7
14. Kumar AS, Durai AR, Sornakumar T (2006) The effect of tool wear on tool life of alumina-based ceramic cutting tools while machining hardened martensitic stainless steel. J Mater Process Technol 173:151–156. doi:10.1016/j.jmatprotec.2005.11.012
15. Zheng G, Zhao J, Gao Z, Cao Q (2012) Cutting performance and wear mechanisms of sialon–Si_3N_4 graded nanocomposite ceramic cutting tools. Int J Adv Manuf Technol 58:19–28. doi:10.1007/s00170-011-3379-2

16. Kübler J, Eblagon F, Graule T, Ehrle B (2008) Development of ceramic composites for industrial wood-cutting tools [J]. Key Engineering Materials 368–372(s 1–2):1062–1067. doi:10.4028/www.scientific.net/KEM.368-372.1062
17. Vagnorius Z, Sørby K (2011) Effect of high-pressure cooling on life of SiAlON tools in machining of Inconel 718. Int J Adv Manuf Technol 54:83–92. doi:10.1007/s00170-010-2944-4
18. Kuzu AT, Bakkal M (2014) The effect of cutting parameters and tool geometry on machinability of cotton-fiber reinforced polymer composites: cutting forces, burr formation, and chip morphology. J Ind Text. doi:10.1177/1528083714560253
19. Yuan S, Zhang C, Amin M, Fan H, Liu M (2015) Development of a cutting force prediction model based on brittle fracture for carbon fiber reinforced polymers for rotary ultrasonic drilling. Int J Adv Manuf Technol 81:1223–1231. doi:10.1007/s00170-015-7269-x
20. Guo X, Ekevad M, Marklund B, Li R, Cao P, Grönlund A (2014) Cutting forces and chip morphology during wood plastic composites orthogonal cutting. Bioresources 9:2090–2106. doi:10.15376/biores.9.2.2090-2106
21. Kumar AS, Durai AR, Sornakumar T (2006) Wear behaviour of alumina based ceramic cutting tools on machining steels. Tribol Int 39:191–197. doi:10.1016/j.triboint.2005.01.021
22. Tian X, Zhao J, Zhao J, Gong Z, Dong Y (2013) Effect of cutting speed on cutting forces and wear mechanisms in high-speed face milling of Inconel 718 with sialon ceramic tools. Int J Adv Manuf Technol 69:2669–2678. doi:10.1007/s00170-013-5206-4
23. Yin YS, Chen SG, Chang XT, Lau AKT (2007) Preparation and mechanical properties of nanocobalt coated Al_2O_3-TiC composites. Key Eng Mater 334-335:913–916. doi:10.4028/www.scientific.net/KEM.334-335.913